Propagation Rate Coefficient of Poly(*N*-isopropylacrylamide) in Water below Its Lower Critical Solution Temperature

François Ganachaud,[†] Robert Balic,[‡] M. J. Monteiro,[§] and R. G. Gilbert*

Key Centre for Polymer Colloids, Chemistry School, Sydney University, NSW 2006, Australia

Received April 7, 2000; Revised Manuscript Received August 28, 2000

ABSTRACT: Pulsed laser polymerization (PLP) of *N*-isopropylacrylamide (NIPAM) in water was performed over the range 2−20 °C (below its lower critical solution temperature), to obtain propagation rate coefficients (k_p). While the value of k_p deduced from these data obeyed some of the consistency criteria for PLP (e.g., that the multiple points of inflection give the same apparent value of k_p), the apparent k_p so obtained depended on monomer and initiator concentrations. For monomer concentration ~0.4−0.8 M, the temperature dependence is approximated by k_p(apparent)/dm^3 mol^{-1} s^{-1} = $10^{8.7}$ exp(−24.5 kJ mol^{-1}/RT). FTIR and osmometry measurements were used to infer the presence of significant amounts of dimer and to deduce the equilibrium constant for dimer formation. A model based on dimerization was derived to account for k_p variations with monomer concentration but did not fit the experimental data, implying that a more complex treatment taking into account complexation with propagating chain ends or a bootstrap effect is required.

Introduction

Knowledge of rate parameters is essential for creating "designed" microstructures in free-radical polymerization. One important parameter is the propagation rate coefficient, k_p. With the advent of pulsed laser polymerization (PLP; for recent reviews, see refs 1−5), accurate k_p values can be determined for a wide range of vinyl monomers. The basic idea of PLP is as follows. Monomer (solution) and photoinitiator are irradiated by pulsed irradiation. Under favorable conditions a significant number of polymer chains which were initiated during one pulse will terminate with a short radical produced during the subsequent pulse, and others will be terminated by the second, third, ..., pulse. The degree of polymerization of the polymer chain terminated "instantaneously" by a radical generated by the nth pulse will be a value L_n given by

$$L_n = nk_p[\mathrm{M}]t \qquad (1)$$

where [M] is the monomer concentration and t is the "dark" time between pulses (t^{-1} is the laser pulse frequency). Modeling molecular weight distributions under various conditions has shown[6−13] that L_n corresponds closely (but not exactly) to a point of inflection on the GPC distribution w(log M).

Although the technique is robust and simple, it is essential that the various criteria for reliability of the value of k_p so obtained, identified by an IUPAC Working Party,[4,5,14] be obeyed (a point which is discussed in detail later). For example, data may be vitiated if the rates of chain transfer (especially to polymer, e.g.,[15] a backbiting reaction which cannot be avoided even at low conversion but can be avoided at low temperatures[16]) influence the molecular weight distribution (MWD) of the PLP sample: vinyl esters and acrylates exhibit a high rate of transfer to polymer, and a high pulse frequency and/or low temperature is required to minimize these effects on the MWD.[16,17]

Attempts have been made to apply PLP to polar monomers propagating in water, such as acrylic and methacrylic acids,[18] (meth)acrylamide,[19] and *N*-isopropylacrylamide (NIPAM).[20] Unfortunately, published PLP k_p data for water-soluble monomers are not yet reliable and/or depend on quantities such as monomer concentration (and thus should be deemed *apparent* rate coefficients), for many different reasons:

(i) Due to their polarity, these monomers are often insoluble in THF, and thus either water-phase GPC must be used, which is well-known to be subject to artifacts, or polymers must be derivatized, e.g., to poly(methyl methacrylate) before GPC analysis,[21] which again is subject to artifacts (e.g., it is difficult to obtain totally quantitative conversion).

(ii) Values of k_p so obtained may depend on factors that should not play a role in the propagation reaction, such as monomer concentration (e.g., as reported for acrylamide[19] and methacrylic acid[18]).

(iii) A strong solvent effect has been observed in polar media, water exhibiting the greatest influence.[22]

(iv) In addition to such technical issues, many of these data do not fulfill IUPAC recommendations[23] that k_p determination should be independent of initiator concentration.

For example, acrylamide PLP data[19] were obtained prior to the development of reliable PLP criteria by the IUPAC Working Party, and tests such as the independence of apparent k_p on laser pulse frequency were not carried out. Thus, the early acrylamide PLP k_p values reported by Pascal et al.[19] cannot be deemed reliable until such checks are performed.

The variations of apparent k_p values determined for water-soluble monomers have been tentatively explained either by the formation of dimers with different propagation rate coefficients or by the presence of

[†] Present address: Laboratoire de Chimie Macromoléculaire, UMR7610, Université Pierre et Marie Curie, Tour 44, 4 Place Jussieu, 75252 Paris cedex 05, France.

[‡] Present address: Dulux Australia, PO Box 60, Clayton South, Vic 3169, Australia.

[§] Present address: Department of Polymer Chemistry & Technology, Eindhoven University of Technology, P.O. Box 513, 5600 MP Eindhoven, The Netherlands.

* Author for correspondence and proofs.

10.1021/ma000619l CCC: $19.00 © 2000 American Chemical Society
Published on Web 10/25/2000

aggregates that partially compartmentalizes the monomer. An aggregation process has also been invoked in a previous paper by the present authors to explain the strange THF-based GPC behavior of this polymer.[24]

The purpose of this article is to measure k_p of NIPAM below its lower critical solution temperature (LCST). It is well established that the aqueous-phase polymerization of highly polar monomers such as NIPAM can be complicated by aggregation effects such as formation of dimers (or higher aggregates), association between monomer and polymer, and so on. In a previous paper on a qualitative study of PLP on NIPAM,[20] the effects of both initiator and monomer concentrations on k_p were presented; further developments will be reported in this article. The data show that the apparent value of k_p depends on quantities such as monomer concentration, which strongly suggests some sort of aggregation or association effect. For this reason, we also obtain data for the equilibrium between monomer and dimer, and a simple model based on the dimerization of NIPAM in water is tested against the observed k_p variations with monomer concentration.

Experimental Section

Materials. NIPAM (Wako) was recrystallized twice from a benzene/hexane mixture, and its purity was checked by ^{1}H NMR.[24] Two different initiators, uranyl nitrate (Ajax Chemical, Melbourne) and 2,2′-azobis(2-amidinopropane) ("V50", from Wako Chemical GmbH) were used without further purification. Uranyl ions are well-known for photoinitiating acrylamide and other monomers in water.[25] The advantage of using uranyl nitrate in PLP experiments[25,26] is that it exclusively undergoes photodissociation, as opposed to V50 which undergoes both photodissociation and thermal dissociation. V50 was found to reinitiate polymerization while drying the samples for GPC analysis, even in the presence of excess hydroquinone, to form new polymer chains that would complicate GPC analysis. Hydroquinone as an inhibitor and distilled water (Milli-Q from Prolabo Instruments) were used without further purification. THF was AR grade (Unichrom).

PLP. Two different devices were used in the PLP experiments: (i) a Nd:YAG laser (Continuum Surelite I-20) with a harmonic generator (Surelite SLD-1 and SLT in series) which produces a 355 nm UV laser radiation; (ii) an excimer XeCl (Lambda Physik, Lextra-200) producing a 308 nm UV radiation. One milliliter samples, containing different amounts of NIPAM and water-soluble initiator, were placed in a precooled brass container and allowed to stand for 4 min before irradiation. In most cases, the polymerization rate was extremely high, and only short irradiation times were required (between 25 and 200 pulses). After laser irradiation, a large excess of hydroquinone (0.5 mL of a 5% w/w aqueous solution) was quickly injected in the cell, which led to the precipitation of the polymer as well as stopping further polymerization. All experiments were carried out in unbuffered water; as the monomer is uncharged, it is expected that the pH is always close to 7 (although it is noted that effects such as the dependence of the apparent k_p on monomer concentration seen here suggest that the apparent k_p will also depend on pH and on ionic strength).

GPC. As described elsewhere,[24] pNIPAM samples need special preparation prior to GPC injection to obtain reliable results. Briefly, the precipitated polymer was totally redissolved in an excess of water and dried in a vacuum oven at 60 °C (above its LCST). The solutions rapidly turned cloudy, and the samples were removed from the oven, when the turbidity disappeared. (The polymer after drying contained enough water molecules solvating the amide groups to redissolve easily in THF.)

The GPC device comprised a Waters 210 pump, a differential refractometer (Waters R401), and a control module to set the temperature (typically 27 °C). Two columns were used in series: Ultrastyragel (Waters), linear, and 10^3 Å. A 100 μL aliquot of sample at different concentrations was injected twice at a THF flow rate of 0.6 mL min^{-1}. The calibration curve was obtained with 12 different polystyrene standards, from Polymer Laboratories and Waters, and fitted by a third-order polynomial. The absolute pNIPAM MWDs were calculated with universal calibration,[27] using the Mark−Houwink parameters for pNIPAM obtained in the previous paper of this series[24] for low molecular weight (typically below 5×10^4), i.e., $K = 5.75 \times 10^{-5}$ dL g^{-1}, $a = 0.78$.

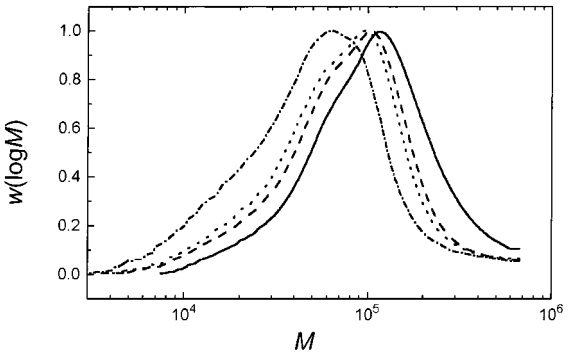

Figure 1. GPC distributions of poly(NIPAM) produced by pulsed laser polymerization at 10 °C, 20 Hz, with different uranyl nitrate concentrations: (—) 0.002, (– – –) 0.005, (···) 0.01, and (– · –) 0.03 M.

FTIR. Some FTIR measurements to quantify the amount of dimer present in a monomer solution were conducted on a BioRad FTS40 device, using an ATR−FTIR cell. NIPAM solutions were freshly prepared before scanning. The region of interest corresponds to the ⟩C═0 and C═C region, located between 1500 and 1700 cm^{-1}. The procedures of deconvolution, smoothing, and integration of the ⟩C═O peaks to find intensity ratios were checked by comparing the C═C peak area, normalized by the monomer concentration, to that from the total amount in dimer plus monomer obtained by deconvolution.

Osmometry. As part of the measurement of the equilibrium constant for dimerization of monomer, the solute content of the NIPAM solution was determined by the osmotic stress method.[28] Two similar round open cells, both topped by a glass narrow capillary and separated by a thin membrane, were screwed together tightly to prevent leaks. The membrane used in these experiments was chosen so that its cutoff was well below the hydrodynamic volume of the NIPAM molecules in these samples. Because this membrane is not stiff enough, it was placed between two layers of a thicker membrane (that commonly used for latex dialysis) for mechanical support.

A 6 mL aliquot of NIPAM solution at a given concentration was first introduced in each cell, and the difference in height between the two capillaries was measured; when the heights are equal, one has equal osmotic pressure. Then the same NIPAM solution was compared to standard solutions of poly(ethylene glycol), PEG, with molecular weight 200 (Fluka AG) at different concentrations.[28] The concentration of the PEG 200 solution with nil osmotic pressure difference corresponds to the amount of solute in the NIPAM solutions.

Results and Discussion

PLP Results. A summary of all PLP experiments is given in Table 1. Typical GPC distributions are shown in Figure 1 and their derivatives (which show the points of inflection) in Figure 2. The recommendations from the IUPAC Working Party[4,5,14] state that the k_p should be independent of one or more of laser frequency, intensity, and wavelength, monomer and initiator concentrations, number of pulses, and initiator type and by the appearance of higher overtones at appropriate multiples of the first point of inflection. Some of these criteria were fulfilled for these NIPAM PLP experi-

Table 1. Summary of PLP Conditions and Deduced Apparent k_p[a]

run	repetition rate (Hz)	temp (°C)	no. of pulses	[M] (M)	[I] (M)	energy per pulse (mJ)	peak mol wt	overtone ratio	apparent k_p ($dm^3\ mol^{-1}\ s^{-1}$)
1	**20**	**20**	50	**0.4**	0.005	29	63 430	0.40	28 065
2	**30**	**20**	100	**0.8**	0.005	29	67 810	0.36	22 505
3	**25**	**26**	50	**0.4**	0.005	29	58 910	0.38	32 580
4	**30**	**26**	50	**0.8**	0.005	29	52 340	0.31	17 370
5	**20**	**10**	50	**0.8**	0.005	29	74 980	0.38	16 590
6	**20**	**2**	50	**0.8**	0.005	29	40 920		9 050
7	**20**	**6.5**	50	**0.8**	0.005	29	46 780	0.50	10 350
8	**30**	**6.5**	50	**0.4**	0.005	29	18 880	0.36	12 530
9	**20**	**15**	50	**0.8**	0.005	29	90 630		20 050
10*	30	**4.6**	200	**0.4**	**0.010**	14.4	22 840	0.31	15 160
11	30	**4.6**	200	**0.4**	**0.010**	14.4	23 950	0.35	15 895
12	30	**4.6**	200	**0.4**	**0.002**	14.4	25 400	0.36	16 860
13	30	**4.6**	200	**0.8**	**0.010**	14.4	27 670	0.41	9 180
14	30	**4.6**	200	**0.8**	**0.002**	14.4	44 660	0.41	14 820
15	30	**8**	200	**0.4**	**0.010**	14.4	20 430	0.29	13 560
16	30	**8**	200	**0.4**	**0.010**	14.4	24 850	0.38	16 495
17	30	**8**	200	**0.4**	**0.002**	14.4	25 310	0.41	16 800
19*	30	**8**	200	**0.8**	**0.002**	14.4	51 020	0.26	16 930
20	30	**12**	200	**0.4**	**0.010**	14.4	26 740	0.37	17 745
21	30	**12**	200	**0.4**	**0.010**	14.4	25 690	0.44	17 050
22	30	**12**	200	**0.4**	**0.002**	14.4	28 170	0.39	18 700
23	30	**12**	200	**0.8**	**0.010**	14.4	50 820		16 865
24*	30	**12**	200	**0.8**	**0.002**	14.4	52 550		17 440
25	30	**17.5**	200	**0.4**	**0.010**	14.4	30 370	0.53	20 155
26	30	**17.5**	200	**0.4**	**0.010**	14.4	29 760	0.52	19 750
27	30	**17.5**	200	**0.4**	**0.002**	14.4	28 070	0.52	18 630
28	30	**17.5**	200	**0.8**	**0.010**	14.4	59 380		19 705
29*	30	**17.5**	200	**0.8**	**0.002**	14.4	55 870		18 540
30	30	**23**	200	**0.4**	**0.010**	14.4	30 300	0.53	20 115
31	30	**23**	200	**0.4**	**0.010**	14.4	28 940	0.57	19 210
32	30	**23**	200	**0.4**	**0.002**	14.4	26 430		17 545
33	30	**23**	200	**0.8**	**0.010**	14.4	44 230		14 675
34	30	**23**	200	**0.8**	**0.002**	14.4	58 870		19 535
35§	20	10	200	**0.08**	0.010	31	33 060		73 150
36§	20	10	200	**0.08**	0.010	31	31 670	0.41	70 060
37§	20	10	200	**0.08**	0.010	31	31 101	0.39	68 808
38§	20	10	200	**0.2**	0.010	31	33 310	0.43	29 480
39§	20	10	200	**0.2**	0.010	31	30 010	0.41	26 560
40§	20	10	200	**0.2**	0.010	31	29 160	0.39	25 800
41§	20	10	200	**0.32**	0.010	31	37 600		20 795
42§	20	10	200	0.32	**0.002**	31	47 430	0.51	26 230
43§	20	10	200	0.32	**0.002**	31	49 030	0.57	27 115
44§	20	10	200	0.32	**0.005**	31	43 850	0.52	24 255
45§	20	10	200	0.32	**0.005**	31	42 750	0.51	23 645
46§	20	10	200	0.32	**0.010**	31	37 010	0.44	20 465
47§	20	10	200	0.32	**0.030**	31	37 000	0.48	20 465
48§	20	10	200	0.32	**0.030**	31	34 450	0.43	19 055
49†§	20	10	200	0.32	$\mathbf{0.004_5}$	31	39 250	0.50	21 710
50†§	20	10	200	0.32	$\mathbf{0.008_5}$	31	37 930	0.44	20 980
51†§	20	10	200	0.32	$\mathbf{0.008_5}$	31	38 783	0.40	21 450
52†§	20	10	200	0.32	**0.014**	31	36 900	0.34	20 410
53†§	20	10	200	0.32	**0.014**	31	39 360	0.35	21 765
54†§	20	10	200	0.32	$\mathbf{0.025_5}$	31	34 670	0.37	19 175
55†§	20	10	200	0.32	$\mathbf{0.025_5}$	31	34 110	0.28	18 865

[a] Entries in bold highlight the parameter that were varied. The overtone ratio is that of the molecular weights at first and second points of inflection (if the latter was observed); one of the PLP consistency criteria is that this ratio should be 0.5. All experiments initiated with uranyl nitrate, except the last runs with the symbol †. All experiments performed with a laser wavelength of 308 nm, except those indicated with the symbol§. *No addition of inhibitor (hydroquinone) at completion of irradiation.

ments. For instance, the laser wavelength (355 or 308 nm) had no effect on the PLP results.

Increasing the number of pulses raised the conversion, leading to more accurate GPC analyses, but showed no apparent systematic effect on k_p values (Table 2). These data were obtained under different GPC conditions from those in Table 1 (only one column) but yield apparent k_p values that are consistent with those in Table 1 for corresponding conditions. In addition, in almost every case, the first and second inflection points were resolved (see Figure 2), and indeed the apparent values of k_p from these first and second points were very close, showing that this consistency check was generally satisfied (Table 1). A second consistency test, the independence of the apparent k_p with pulse frequency, was not systematically examined. Discrepancies arise from a third consistency test: the variation of the apparent k_p values with varying concentrations of initiator and monomer, as discussed below.

Influence of Initiator Type and Concentration. Figure 1 shows the effect of the amount of initiator on the GPC distribution. The GPC chromatograms vary greatly in shape with the concentration of initiator. For low initiator concentrations, the first inflection point is lower than the second (Figure 1). The appearance of a second maximum can be ascribed to a slow termination

Table 2. Data to Check Any Systematic Variation of the Apparent k_p with Number of Pulses

repetition rate (Hz)	temp (°C)	no. of pulses	[M] (M)	[I] (M)	energy per pulse (mJ)	peak mol wt	overtone ratio	apparent k_p ($dm^3\ mol^{-1}\ s^{-1}$)
30	10	50	0.4	0.01	27.9	18 150	0.42	12 050
30	10	25	0.4	0.01	27.9	19 150	0.44	12 710
30	10	35	0.4	0.01	27.9	19 360	0.46	12 850
30	10	100	0.4	0.005	27.9	18 050	0.46	11 980
30	10	50	0.4	0.005	27.9	19 300	0.49	12 810
30	10	25	0.4	0.005	27.9	18 950	0.42	12 570
30	10	35	0.4	0.005	27.9	18 330	0.38	12 170
30	10	100	0.4	0.001	27.9	19 760	0.49	13 120
30	10	50	0.4	0.001	27.9	19 630	0.50	13 030
30	10	25	0.4	0.001	27.9	19 730	0.48	13 100
30	10	35	0.4	0.001	27.9	21 070	0.49	13 980

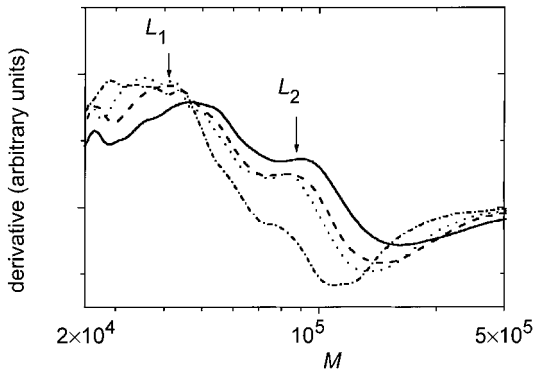

Figure 2. Derivative of the data of Figure 1, where the maxima show the molecular weights corresponding to the points of inflection in Figure 1; one of the PLP criteria is that higher overtones (higher points of inflection) should give the same apparent k_p as the first point of inflection (eq 1).

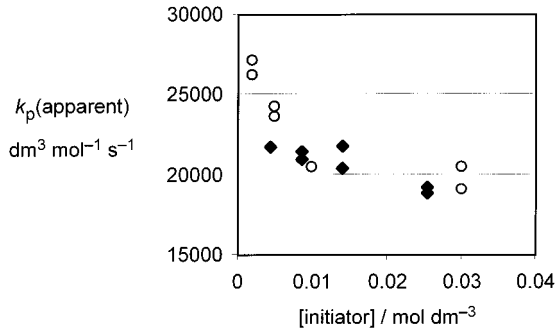

Figure 3. Influence of the type and initiator concentration on the apparent k_p values: (○) uranyl nitrate; (◆) V50. PLP conditions: frequency 20 Hz, monomer concentration 0.32 M, temperature 10 °C.

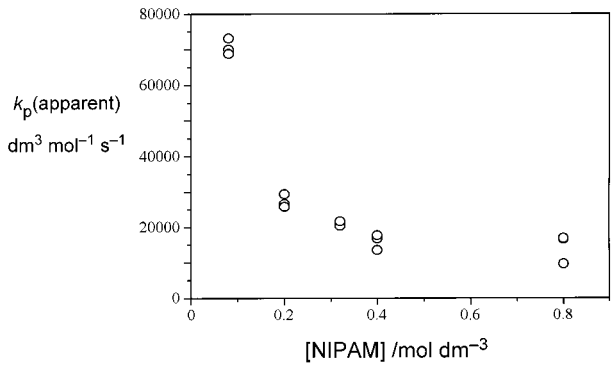

Figure 4. Influence of the monomer concentration on the apparent k_p. PLP conditions: frequency 20 Hz, [uranyl nitrate] = 0.01 M, temperature = 8−12 °C.

rate, such that the majority of propagating chains terminates between pulses rather than at each pulse.[20] This behavior has been described in an article reviewing the PLP conditions for vinyl acetate.[11] Raising the initiator concentration increases the amount of radicals created at each pulse, which in turn promotes "immediate" termination. This is the case here, as the first peak becomes dominant with increasing initiator concentration.

This shape variation also influences the value of the overtone ratio (Table 1), defined as the ratio of k_p calculated using the molecular weight at the first and second inflection points. The IUPAC Working Party[4,5,14] stated that in reliable PLP experiments this ratio should ≈0.50. As demonstrated by Buback et al.,[29] this quantity varies proportionally to the ratio of the first and second maxima (or inflection point, when peaks are not resolved enough). It has been suggested[29] that these discrepancies are due to SEC broadening.

The effect of the type and concentration of initiator was examined at 10 °C, with frequency 20 Hz and fixed monomer concentration (0.32 M, runs 41−54). Significant variations of the k_p values were observed with initiator concentration, especially with uranyl nitrate (Figure 3). The same trend has also been observed at 30 Hz and with uranyl nitrate as the initiator, but to a lesser extent (Table 2).[20] It is possible that a higher pulse repetition rate would lead to better-resolved molecular weight distributions, as seen elsewhere.[16,30,31]

Influence of Monomer Concentration. It has been reported in the literature that k_p values (obtained by PLP) in nonaqueous solvents generally are only slightly influenced by solvent,[32−36] although there are a few instances where such effects are significant: where the interaction of the solvent with monomer and/or polymer is unusually strong.[32,37] However, the present *aqueous* system shows a large variation of apparent k_p with monomer concentration, as shown in Figure 4 (20 Hz, uranyl nitrate as initiator, temperature range 8−10 °C). It can be seen from this plot that an increase in monomer concentration results in a decrease in k_p, a similar but more pronounced effect to that observed for initiator concentration (Figure 3).

In previous studies of k_p for methacrylic acid,[18,21] the only system showing a significant solvent effect was water, which also showed a decrease of apparent k_p with monomer concentration.[18] Water solvation, which is believed to play an important role in the propagation step of polar monomers, depends strongly on the concentration of all species (monomer, initiator, salt, and solvent) in the mixture. The present system clearly also exhibits a strong solvent effect.

Apparent Arrhenius Parameters. An Arrhenius plot of the k_p data for NIPAM concentration of 0.4 and 0.8 M (where apparent k_p's are almost constant with monomer concentration) is given in Figure 5. As re-

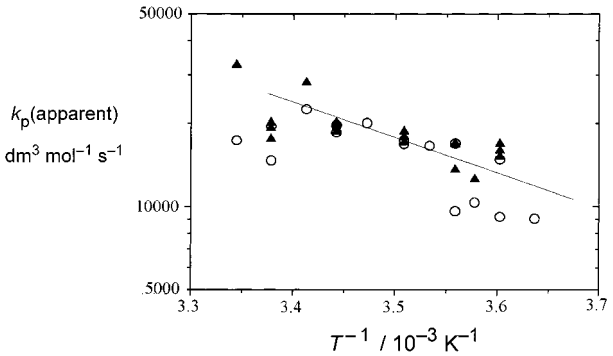

Figure 5. Arrhenius plot of all the data for [NIPAM] of 0.4 (▲) and 0.8 M (○), from Table 1. Line: best fit between 2 and 20 °C.

ported elsewhere,[20] the value of k_p seems to level off at higher temperatures, which may be because transfer reactions influence the MWD. However, the large scatter in the data and the small temperature range, along with the strong solvent effect, imply that no reliable inferences can be drawn from this Arrhenius plot. Arrhenius parameters were calculated between 2 and 20 °C: k_p(apparent)/dm^3 mol^{-1} s^{-1} = $10^{8.7}$ exp(−24.5 kJ mol^{-1}/RT). The apparent activation energy and preexponential factor lie within the range commonly encountered for vinyl monomers.

Effect of Dimerization

In the following part, a simple treatment is proposed to describe and account for dimerization effects. Measurements of the equilibrium between monomer and dimer were performed at 10 and 25 °C.

Basic Assumptions. The ability of some monomers to form dimers in different polar media has already been reported.[21] Dimers form when solvency decreases, for instance by increasing salt or monomer concentrations. The dimer association equilibrium constant, K_{dim}, is

$$K_{dim} = \frac{[D]}{[M]^2} \tag{2}$$

where [M] and [D] are monomer and dimer concentrations, respectively. $[M]_T$, the overall NIPAM concentration, is then given by

$$[M]_T = [M] + 2[D] \tag{3}$$

The solution of eqs 2 and 3 is

$$[M] = \frac{\sqrt{1 + 8K_{dim}[M]_T} - 1}{4K_{dim}} \tag{4}$$

Experimental evidence for dimerization in other water-soluble monomers (methacrylic acid, acrylamide) has been obtained by FTIR.[19,21] In the present work, FTIR and osmometry are used to determine K_{dim}, as described in the next subsection. Attempts were also made to use ^{1}H NMR to determine the ratio of dimer to monomer concentrations by following the variation of the double-bond peak with monomer concentration; good signals could not be obtained, perhaps because the interchange between monomer and dimer is too fast to be measured on the NMR time scale.

Determination of Dimer Association Constant from FTIR Studies. FTIR spectra of NIPAM at different concentrations in water (without added initiator or polymer) are given in Figure 6. Each spectrum has been normalized (i.e., divided by the actual monomer concentration). Identification of the peaks was carried out using the method suggested by Beuermann et al.[21] for methacrylic acid, where it was shown that the position of the double-bond peak does not vary with the solution concentration (left peak, Figure 6).

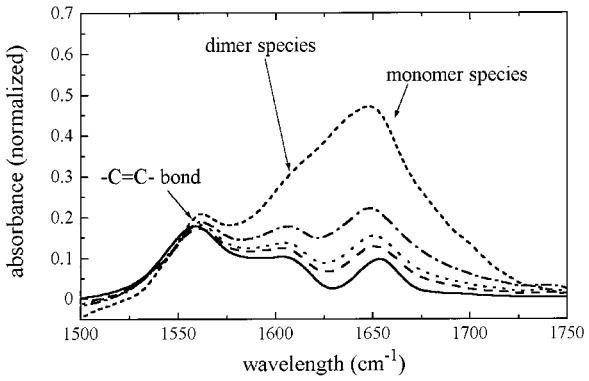

Figure 6. FTIR spectra of NIPAM at different concentrations in deionized water: (—) 0.8, (– – –) 0.4, (· · ·) 0.32, (– · –) 0.2, (···) 0.08 M.

Table 3. FTIR and Osmometry Results

$[M]_T$ (M)	R(FTIR)	[S] (M) (osmometry)	$[M]_T$ (M)	R(FTIR)	[S] (M) (osmometry)
0.08	0.00	0.058	0.40	0.51	0.328
0.20	0.11	0.147	0.80	0.78	0.612
0.32	0.28		0.80[a]		0.543

[a] This solution contained 0.010 M of uranyl nitrate.

Values of the dimer/monomer ratio were obtained by deconvolution and integration of the peaks. The variation in the amount of dimer with [NIPAM] is given in Table 3.

The dimer/monomer intensity ratio R obtained from FTIR is found using

$$R = \frac{\epsilon_D[D]}{\epsilon_M[M]} \tag{5}$$

where ϵ_D and ϵ_M are the absorbances of dimer and monomer, respectively. Equations 2−5 yield

$$R = \frac{\epsilon_D}{4\epsilon_M}\left(\sqrt{1 + 8K_{dim}[M]_T} - 1\right) \tag{6}$$

Observed values of R as a function of total monomer concentration can then be fitted by nonlinear least-squares to yield K_{dim}. A convenient alternative to this fitting procedure is to look at the limit of high amounts of monomer. One has

$$R \approx \frac{\epsilon_D}{\epsilon_M}\left(\frac{K_{dim}}{2}\right)^{1/2}\sqrt{[M]_T} - \frac{\epsilon_D}{4\epsilon_M}, \quad [M]_T \gg \frac{1}{8K_{dim}} \tag{7}$$

Equation 7 shows that a plot of R as a function of $[M]_T^{1/2}$ should yield a straight line whose slope will give $K_{dim}^{1/2}$, which provides a convenient means to estimate this quantity. Figure 7 shows the low- and high-concentration limiting behaviors and the fit using the value of K_{dim} found fitting the data to eq 7 and to the complete

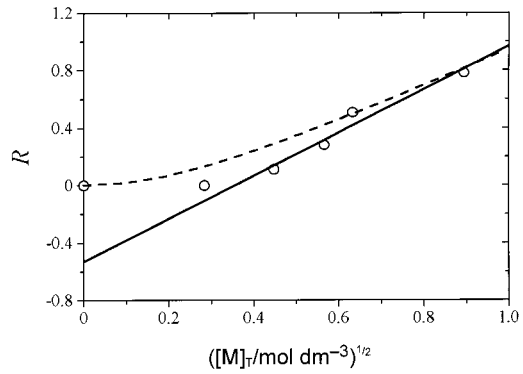

Figure 7. Points: observed value of the intensity ratio R (eq 5) as a function of total monomer concentration. Full line: fit using approximate form, eq 7; dotted line, fit with full form, eq 6, using $\epsilon_D/\epsilon_M = 1.9$, $K_{dim} = 1.0\ M^{-1}$.

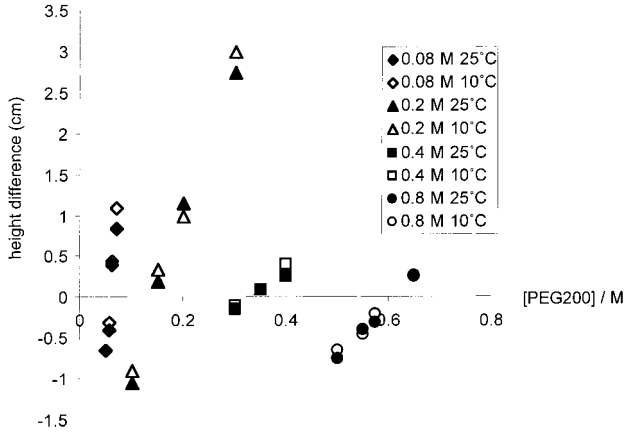

Figure 8. Osmometry data: height differences at two temperatures as a function of the concentration of PEG 200, at 10 and 25 °C, for a range of concentrations of NIPAM (no added electrolyte).

form of eq 6. This gives $K_{dim} = 1.0\ M^{-1}$. The agreement between the fit and the experimental points is acceptable.

Dimer Association Constant from Osmometry. The osmotic stress method[28] involves measuring the difference in osmotic pressure of two solutions separated by a very low cutoff dialysis membrane. A standard is chosen which is known not to dimerize and is of almost the same molecular weight as the monomer/dimer NIPAM; poly(ethylene glycol) (PEG) of molecular weight 200 was chosen for this purpose.[28] One cell is filled with a NIPAM solution and the other one with a standard solution. The PEG concentration is varied so as to reach a similar osmotic pressure in the two cells. The osmotic pressure, π, is proportional to the amount of solute [S] present in the samples, and calibration is made with PEG of known concentration. Results (height difference as a function of PEG concentration) are shown in Figure 8 for a range of samples with different [NIPAM] concentrations, at both 10 and 25 °C.

The osmotic pressure data are then used to obtain the equilibrium constant as follows. One has

$$[S] = [M] + [D] \tag{8}$$

or, using eqs 2 and 3,

$$[S] = {}^1/_2[M]_T + \frac{\sqrt{1 + 8K_{dim}[M]_T} - 1}{8K_{dim}} \tag{9}$$

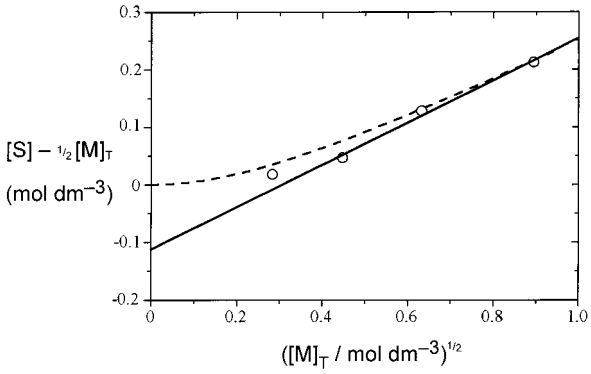

Figure 9. Points: plot of $[S] - {}^1/_2[M]_T$ (from osmotic pressure data) as a function of $[M]_T^{1/2}$ (see eq 10). Full line: line of best fit using eq 10; broken line: calculated from eq 9 using $K_{dim} = 1.0\ M^{-1}$ (obtained from FTIR data of Figure 6).

Table 4. Experimental Results for Dimer Association Constant K_{dim} (No Added Initiator or Other Salt, 10 and 25 °C)

method	K_{dim}/M^{-1}
FTIR	1.00
osmometry (from slope)	1.11
osmometry (from intercept)	0.93

Again, the high-concentration limit is

$$[S] - {}^1/_2[M]_T \approx \sqrt{\frac{[M]_T}{8K_{dim}}} - \frac{1}{8K_{dim}}, \quad [M]_T \gg \frac{1}{8K_{dim}} \tag{10}$$

The value of [S] is obtained from the observed values of π. Hence, the slope and intercept of a plot of $[S] - {}^1/_2[M]_T$ as a function of $[M]_T^{1/2}$ should yield independent values of K_{dim}. This method thus has an internal consistency check. Results are reported in Table 3 for different NIPAM concentrations and are plotted in Figure 9. As seen in Table 4, values of K_{dim} from all three methods (FTIR and slope and intercept of osmometry values) are in accord.

It is apparent from Figure 8 that, for a given NIPAM concentration, there is apparently no significant temperature variation in the PEG reference concentration at which the height difference is zero; i.e., there is apparently no significant temperature variation in the K_{dim} as inferred from the osmometry data. This result is unexpected. One possible explanation is that there is an accidental cancellation in enthalpic effects of NIPAM−NIPAM, NIPAM−water, and water−water interactions, at least under the present conditions.

The data reported for K_{dim} up to this point are for systems with no added salt. However, there is a significant influence of ionic strength on value of this quantity. A concentrated solution of NIPAM (0.8 M) containing a typical amount of uranyl initiator used in the PLP experiments (0.010 M) was prepared and the amount of solute determined by osmometry (see Table 3). This solution gave a value of $K_{dim} = 3.8\ M^{-1}$. This is significantly larger than that determined without added salt (i.e., initiator). Again, there is no significant temperature variation in this quantity over the range 10−25 °C.

This value of the association equilibrium constant predicts that, at the highest concentration of added monomer (0.8 M) in the presence of 0.01 M UO_2^{2+}, the fraction of dimer, [D]/([M] + [D]), is 33%.

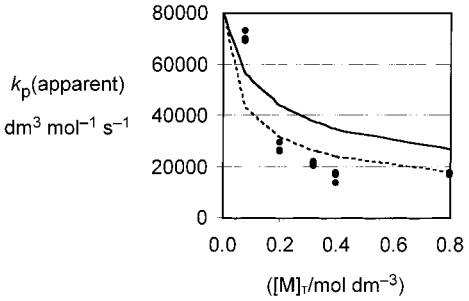

Figure 10. Lines: calculated dependence of k_p on total amount of added monomer, using eq 12, with $K_{dim} = 3.8$ (full line) and 10 M^{-1} (broken line), $k_{pM} = 8 \times 10^4$ dm^3 mol^{-1} s^{-1}, $k_{pD} = 10^3$ dm^3 mol^{-1} s^{-1}; points: data of Figure 4.

Dimerization and NIPAM Propagation. The simplest possible way of accounting for the effect of dimer formation on the apparent value of k_p would be to assume that encounter of a radical with a dimer means a much higher local concentration of monomer. However, this would predict that k_p would increase with [NIPAM] (increased local concentration), whereas the reverse is observed (Figure 4). Although it has been inferred[38] that dimers are more reactive than monomers, in fact an increased rate effect with increased amount of dimer may be due to a different local concentration and/or a different propagation rate coefficient.

We now present and then test a more sophisticated model for the effect of dimer on the apparent value of k_p. It is assumed that monomer and dimer propagate with different propagation rate coefficients, k_{pM} and k_{pD}, respectively.[19] In addition, it is assumed that there is only one type of polymeric radical species propagating with either the monomer or dimer:

$$\sim M_n^{\bullet} + M \xrightarrow{k_{pM}} \sim M_{n+1}^{\bullet}$$

$$\sim M_n^{\bullet} + D \xrightarrow{k_{pD}} \sim M_{n+1}^{\bullet} + M$$

Here, propagation of dimer is assumed to result in the release of a monomer molecule. The apparent value of k_p is thus given by

$$k_{p,app}[M]_T = k_{pM}[M] + k_{pD}[D] \qquad (11)$$

Using eqs 2 and 3, one has

$$k_{p,app} = {}^1/_2 k_{pD} - ({}^1/_2 k_{pD} - k_{pM}) \frac{\sqrt{1 + 8K_{dim}[M]_T} - 1}{4K_{dim}[M]_T} \qquad (12)$$

Figure 10 shows the calculated dependence of $k_{p,app}$ on total amount of added monomer, for fixed K_{dim}, predicted by eq 12; this has the same qualitative form (a monotonic decrease) as the data of Figure 4. Moreover, eq 12, together with the experimental observation that K_{dim} increases with increasing ionic strength and hence with initiator concentration, also implies that $k_{p,app}$ also decreases with increasing initiator concentration (for fixed $[M]_T$), qualitatively consistent with the data in Figure 3.

The model can be tested quantitatively against experiment by choosing a value of K_{dim} and plotting the observed value of the apparent k_p against the quantity $\{(1 + 8K_{dim}[M]_T)^{1/2} - 1\}/4K_{dim}[M]_T$, as suggested by eq 12. The intercept of such a plot should then yield k_{pD}, and the sum of the slope and intercept should yield k_{pM}. This plot is shown in Figure 11, using the $k_{p,app}$ data of Figure 4, for a range of values of K_{dim} encompassing that obtained in the preceding section for these conditions (in the presence of 0.1 M uranyl nitrate), $K_{dim} = 3.8$ M^{-1}. It is seen that the data can indeed be fitted by an apparently adequate straight line. However, the intercept is *negative*, which is physically impossible. While it is tempting to discount the largest values of $k_{p,app}$ (whose removal would give a positive intercept) as being the "fliers" in Figure 11, unfortunately these data in fact correspond to the lowest values of monomer concentration, which would give the *least* association effects; it is clearly association effects of some sort which are responsible for the variation of $k_{p,app}$ with monomer concentration.

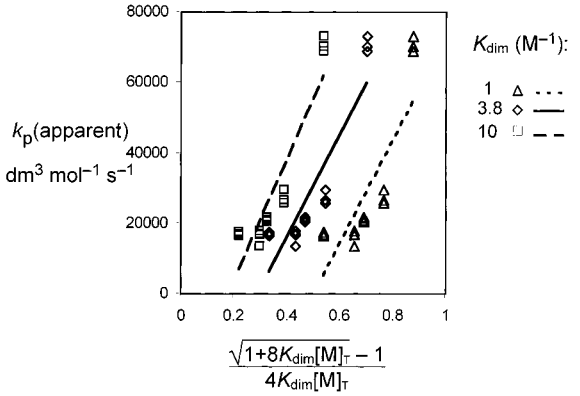

Figure 11. Data for the dependence of the apparent propagation rate coefficient on monomer concentration of Figure 4, plotted as a function of $\{(1 + 8K_{dim}[M]_T)^{1/2} - 1\}/4K_{dim}[M]_T$, as suggested by eq 12, for various values of K_{dim}. Lines: linear least-squares fit.

It is therefore concluded that the dimerization model alone is insufficient to account for the experimentally observed dependence of the apparent propagation rate coefficient on monomer concentration. A more complex model is needed to describe the data, perhaps complexation between monomer and the active polymer chain end[39] ("bootstrapping"[40]) or partial aggregation of the polymer. The latter would be consistent with a recent report[41] on the polymerization of NIPAM in water (below its LCST) followed by a combination of static and dynamic light scattering. This kinetic study showed that there was a compartmentalization effect in such systems, supported by dramatic changes in polymer conformation. The aggregation process was shown to vary with the amount of polymer and monomer present in the aqueous phase, as well as the initial monomer concentration.

Conclusions

Pulsed laser polymerizations of a functional monomer, NIPAM, in water were conducted to gain insight into the complexities of polymerizing water-soluble monomers. The PLP data obey some of the consistency tests for this method, in particular obtaining the same k_p values for higher overtones (chains which are terminated by radicals formed two pulses after the initiating pulse). However, the apparent k_p is affected by the initiator concentration (the uranyl and V-50 photoinitiators are both salts) and by monomer concentration. For a given initiator and monomer concentrations, the

k_p values satisfy the PLP criterion of consistency with values obtained for higher overtones.

This dependence on monomer and salt concentrations can at least in part be ascribed to association effects. One such is the occurrence of dimer. FTIR and osmometry measurements at 10−25 °C yielded a value for the dimer association constant, which showed that up to $\sim^2/_3$ of monomer was present as dimer at the highest monomer concentrations used in these experiments. Two possibilities that in themselves might account for the association effects were discounted: a simple increased local monomer concentration due to the presence of dimer (since this would give the opposite dependence on [monomer] to that observed) and a more complicated model allowing for different propagation rate coefficients for monomer and dimer (which gave the correct qualitative dependence but inconsistent fits to the data when used in conjunction with the measured K_{dim}). Arrhenius parameters calculated between 2 and 20 °C (below the lower critical solution temperature) were in the same (wide) range as for other vinyl monomers: $k_p(\text{apparent})/\text{dm}^3\ \text{mol}^{-1}\ \text{s}^{-1} = 10^{8.7} \exp(-24.5\ \text{kJ mol}^{-1}/RT)$. However, no physical meaning can be ascribed to the activation energy and frequency factors, because of the observed association effects.

A more complex scheme than a simple equilibrium between monomer and dimer is required to account for the observed concentration dependence of the apparent k_p. Complexation with propagating chain ends, in which the local monomer concentration surrounding the propagating chain is not the same as the global monomer concentration, is one possible explanation.

Acknowledgment. F.G. gratefully acknowledges the support of an Australian Research Council International Exchange Fellowship and of an *Innovalyon* award. R.B. gratefully acknowledges the support of a PhD scholarship from Union Carbide. The collaboration of A/Prof Greg Warr in the osmometry measurements is greatly appreciated. The collaboration of Dr. Scott Kable in the laser experiments is also gratefully acknowledged. We especially appreciate the suggestions from Professor Tom Davis which were an essential part of accurately quantifying the molecular weight distributions. The Key Centre for Polymer Colloids is established and supported under the Australian Research Council's Research Centres Program.

References and Notes

(1) Coote, M. L.; Zammit, M. D.; Davis, P. D. *Trends Polym. Sci.* **1996**, *4*, 189.
(2) van Herk, A. M. *J. Macromol. Sci., Rev. Macromol. Chem. Phys.* **1997**, *C37*, 633.
(3) Beuermann, S.; Buback, M.; Davis, T. P.; Gilbert, R. G.; Hutchinson, R. A.; Kajiwara, A.; Klumperman, B.; Russell, G. T. *Macromol. Chem. Phys.* **2000**, *201*, 1355.
(4) Beuermann, S.; Buback, M.; Gilbert, R. G.; Hutchinson, R. A.; Klumpermann, B.; Olaj, F. O.; Russell, G. T.; Schweer, J. *Macromol. Chem. Phys.* **1997**, *198*, 1545.
(5) Gilbert, R. G. *Pure Appl. Chem.* **1996**, *68*, 1491.
(6) Deady, M.; Mau, A. W. H.; Moad, G.; Spurling, T. H. *Makromol. Chem.* **1993**, *194*, 1691.
(7) Olaj, O. F.; Zifferer, G. *Makromol. Chem., Theory Simul.* **1992**, *1*, 71.
(8) Lu, J.; Zhang, H.; Yang, Y. *Macromol. Chem., Theory Simul.* **1993**, *2*, 747.
(9) O'Driscoll, K. F.; Kuindersma, M. E. *Macromol. Theory Simul.* **1994**, *3*, 469.
(10) Hutchinson, R. A.; Aronson, M. T.; Richards, J. R. *Macromolecules* **1993**, *26*, 6410.
(11) Hutchinson, R. A.; Richards, J. R.; Aronson, M. T. *Macromolecules* **1994**, *27*, 4530.
(12) Sarnecki, J.; Schweer, J. *Macromolecules* **1995**, *28*, 4080.
(13) Buback, M.; Busch, M.; Lämmel, R. A. *Macromol. Theory Simul.* **1996**, *5*, 845.
(14) Beuermann, S.; Buback, M. *Pure Appl. Chem.* **1998**, *70*, 1415.
(15) Plessis, C.; Arzamendi, G.; Leiza, J. R.; Schoonbrood, H. A. S.; Charmot, D.; Asua, J. M. *Macromolecules* **2000**, *33*, 4.
(16) Lyons, R. A.; Hutovic, J.; Piton, M. C.; Christie, D. I.; Clay, P. A.; Manders, B. G.; Kable, S. H.; Gilbert, R. G. *Macromolecules* **1996**, *29*, 1918.
(17) Hutchinson, R. A.; Paquet, D. A.; McMinn, J. H. *Macromolecules* **1995**, *28*, 5655.
(18) Kuchta, F.-D.; Van Herk, A. M.; German, A. L. *Macromolecules* **2000**, *33*, 3641.
(19) Pascal, P.; Winnik, M. A.; Napper, D. H.; Gilbert, R. G. *Macromolecules* **1993**, *26*, 4572.
(20) Ganachaud, F.; Monteiro, M. J.; Gilbert, R. G. *Macromol. Symp.* **2000**, *150/151*, 275.
(21) Beuermann, S.; Paquet, D. A.; Mcminn, J. H.; Hutchinson, R. A. *Macromolecules* **1997**, *30*, 194.
(22) Gromov, V. F.; Bune, E. V.; Teleshov, E. N. *Russ. Chem. Rev.* **1994**, *63*, 507.
(23) Buback, M.; Gilbert, R. G.; Hutchinson, R. A.; Klumperman, B.; Kuchta, F.-D.; Manders, B. G.; O'Driscoll, K. F.; Russell, G. T.; Schweer, J. *Macromol. Chem. Phys.* **1995**, *196*, 3267.
(24) Ganachaud, F.; Monteiro, M. J.; Gilbert, R. G.; Dourges, M.-A.; Thang, S. H.; Rizzardo, E. *Macromolecules*, in press.
(25) Venkatarao, K.; Santappa, M. *J. Polym. Sci., Part A-1* **1967**, *5*, 637.
(26) Venkatarao, K.; Santappa, M. *J. Polym. Sci., Part A-1* **1970**, *8*, 3429.
(27) Gallot-Grubisic, Z.; Rempp, P.; Benoit, H. *Polym. Lett.* **1967**, *5*, 753.
(28) Parsegian, V. A.; Rand, R. P.; Fuller, N. L.; Rau, D. C. *Methods Enzymol.* **1986**, *127*, 400.
(29) Buback, M.; Geers, U.; Kurz, C. H.; Heyne, J. *Macromol. Chem. Phys.* **1997**, *198*, 3451.
(30) Buback, M.; Kurz, C. H.; Schmaltz, C. *Macromol. Chem. Phys.* **1998**, *199*, 1721.
(31) Beuermann, S.; Paquet, D. A.; McMinn, J. H.; Hutchinson, R. A. *Macromolecules* **1996**, *29*, 4206.
(32) Zammit, M. D.; Davis, T. P.; Willett, G. D.; O'Driscoll, K. F. *J. Polym. Sci., Part A: Polym. Chem.* **1997**, *35*, 2311.
(33) Olaj, O. F.; Schnoll-Bitai, I. *Mon. Chem.* **1999**, *130*, 731.
(34) Morrison, B. R.; Piton, M. C.; Winnik, M. A.; Gilbert, R. G.; Napper, D. H. *Macromolecules* **1993**, *26*, 4368.
(35) Beuermann, S.; Buback, M.; Schmaltz, C. *Macromolecules* **1998**, *31*, 8069.
(36) Beuermann, S.; Buback, M.; Russell, G. T. *Macromol. Rapid Commun.* **1994**, *15*, 647.
(37) O'Driscoll, K. F.; Monteiro, M. J.; Klumperman, B. *J. Polym. Sci., Part A: Polym. Chem.* **1997**, *35*, 515.
(38) Plochocka, K. *J. Macromol. Sci., Rev. Macromol. Chem.* **1981**, *C20*, 67.
(39) Kamachi, M. *Adv. Polym. Sci.* **1981**, *38*, 55.
(40) Harwood, H. J. *Makromol. Chem., Makromol. Symp.* **1987**, *10/11*, 331.
(41) Norisuye, T.; Shibayama, M.; Nomura, S. *Polymer* **1998**, *39*, 2769.

MA000619L